Available online at www.sciencedirect.com

ScienceDirect

Procedia CIRP 58 (2017) 55 – 60

www.elsevier.com/locate/procedia

16th CIRP Conference on Modelling of Machining Operations

Influence of the cutting edge microgeometry on the surface integrity during mechanical surface modification by Complementary Machining

Michael Gerstenmeyer[a,*], Benjamin-Lars Ort[b], Frederik Zanger[a], Volker Schulze[a]

[a]*Karlsruhe Institute of Technology (KIT), wbk Institute of Production Science, Kaiserstr. 12, 76131 Karlsruhe, Germany*
[b]*Faculty of Mechanical Engineering, Karlsruhe Institute of Technology (KIT), Kaiserstr. 12, 76131 Karlsruhe, Germany*

* Corresponding author. Tel.: +49 721 608-45906; fax: +49 721 608-45004. E-mail address: michael.gerstenmeyer@kit.edu

Abstract

In metal production, mechanical surface modifications are used to optimize workpiece characteristics to improve properties such as fatigue strength. Machining and mechanical surface modification can be integrated in the process strategy Complementary Machining. After machining the cutting tool is used reversely acting as a tool for mechanical surface modification. This paper shows the influence of the cutting edge microgeometry on process forces and temperatures as well as process induced grain refinement in the surface layer during the mechanical surface modification of Armco-Iron and AISI 4140. The mechanical surface modification is simulated in a 3D-FEM-simulation with ABAQUS/Standard.

Keywords: Surface Modification; Cutting Edge; Complementary Machining

1. Introduction

In machining operations of metallic components, it is of great importance to produce surfaces with high geometric accuracy and surface integrity due to the machining process. In this context, surface integrity includes to enhance workpiece characteristics like fatigue strength, wear resistance, tribology or corrosion [1]. The surface layer state (e.g. residual stresses, roughness, micro hardness or grain size) has a significant influence on these workpiece properties [2-5]. During machining the cutting edge microgeometry substantially influences the resulting surface layer states as a result of the impact of high thermal and mechanical loads [6]. For this reason the cutting edge microgeometry and the preparation of these are in focus of research investigations [7-9].

In industrial applications a machining process is followed by a mechanical surface modification processes to improve surface integrity. Mechanical surface modification processes aim to smoothen the surface topography, influence residual stresses, increase the hardness or influence the microstructure. The surface layer states can be achieved by a local plastic deformation of the surface layer during the surface modification.

The process strategy Complementary Machining combines the machining and the mechanical surface modification [10]. After the machining process the cutting tool is used in opposite direction resulting in a plastic deformation of the surface layer. On the one hand, the process is reciprocal because the tools are used in the opposite direction. On the other hand the process is integral because standard machining is supplemented by mechanical surface modification. For that reason the machining strategy is called Complementary Machining. Previous investigations of Complementary Machining showed the reduction of surface roughness and an increased strain hardening [11].

One of the objectives of the current investigation is to generate knowledge about the influence of the cutting edge microgeometry on the resulting process forces, temperatures and microstructure during mechanical surface modification by Complementary Machining of Armco-Iron and AISI 4140. The mechanical surface modification is simulated in a 3D-FEM-simulation with ABAQUS/Standard.

doi:10.1016/j.procir.2017.03.185

2. Setup and Materials

2.1. Cutting edges

To analyze the influence of cutting edge microgeometry on surface integrity, the microgeometry has to be defined. In Fig. 1 the contact conditions between the tool and the workpiece during the mechanical surface modification by Complementary Machining are shown. After the machining process with process parameters cutting velocity v_c and cutting depth h the cutting tool is used in opposite direction for the mechanical surface modification. For the surface modification the penetration depth a_p and the surface modification velocity v_{st} are the characteristic process parameters for this process step.

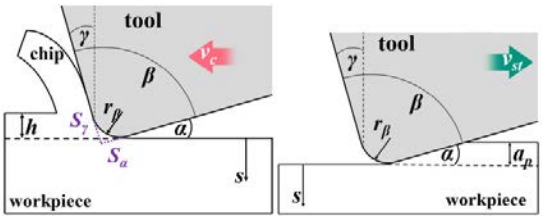

Figure 1. Contact conditions for Complementary Machining

In this paper the microgeometry of the cutting edge is characterized by the form-factor method following the approach of Denkena [12] for the machining process. The form-factor K is defined as

$$K = \frac{S_\gamma}{S_\alpha} \tag{1}$$

S_γ is the cutting edge segment on the rake face, S_α is the cutting edge segment on the flank face. This definition is the basis for machining and surface modification.

2.2. Finite element model

The finite element model is described as a three-dimensional orthogonal cutting process with the FEM software ABAQUS/Standard. The model consists of two bodies, the tool and the workpiece. The tool is defined as a rigid body only allowing the workpiece to be deformed and to be meshed with hexahedral coupled temperature-displacement (C3D8T) elements. The width was fixed at 600 µm and the other geometry parameters varied according to the penetration depth a_p and the form-factor K. The workpiece is defined as a rectangular solid with a width of 500 µm, a length of 700 µm and a height of 300 µm. Moreover it is meshed with tetrahedral coupled temperature-displacement (C3D4T) elements.

During the process the tool moves with the surface modification velocity v_{st} along the fixed workpiece. The microgeometries of the tool are generated through fitting ellipses, determined by S_γ and S_α,. In addition, two sources of heat generation were implemented into the model. On the one hand, heat generation through friction. Therefore, a constant friction coefficient μ was used following the approach of Coulomb's law. On the other hand, heat generation through plastic deformation was implemented. The description of the flow behavior and the grain size of the material model AISI 4140 and Armco-Iron are implemented through a UHARD subroutine into the ABAQUS/Standard model.

2.3. Modelling of flow stress and grain refinement

The flow stress σ depends on the temperature T and the strain rate $\dot{\varepsilon}$. Thereby, the flow stress can be decomposed in an athermal component σ_G and a thermal component $\sigma^*(T,\dot{\varepsilon})$. These are based on the approaches of [13-15].

$$\sigma = \underbrace{\sigma_0^* \cdot \left(1-\left(\frac{T}{T_0}\right)^n\right)^m}_{\sigma^*} + \underbrace{\left(\sigma_{G0} + \left(\sigma_1 + \theta_1 \cdot \overline{\varepsilon_p}\right) \cdot \left(1 - \exp\left(-\frac{\theta_1 \cdot \overline{\varepsilon_p}}{\theta_0}\right)\right)\right) \cdot \frac{G(T)}{G(0K)} \cdot g(T,T_{tr})}_{\sigma_G} \tag{2}$$

Due to short range dislocation obstacles the thermal component $\sigma^*(T,\dot{\varepsilon})$ depends on temperature T, the strain rate $\dot{\varepsilon}$ and the material constants n and m. The thermal component $\sigma^*(T,\dot{\varepsilon})$ increases with decreasing temperature and an increasing strain rate. Above the temperature T_0 the thermal component will be neglected. T_0 is defined as

$$T_0 = \frac{\Delta G_0}{k_B \ln\left(\frac{\dot{\varepsilon}_0}{\dot{\overline{\varepsilon}}_p}\right)} \tag{3}$$

with the free activation enthalpy ΔG_0 and the Boltzmann constant k_B.

Due to long range dislocation obstacles the athermal component σ_G slightly depends on the temperature T and the shear modulus G. The term $g(T,T_{tr})$ describes the high temperature softening and is 1 for $T \leq T_{tr}$. For $T > T_{tr}$, $g(T,T_{tr})$ is defined as

$$g(T,T_{tr}) = \left(1-\left(\frac{T-T_{tr}(\dot{\overline{\varepsilon}}_p)}{T_m - T(\dot{\overline{\varepsilon}}_p)}\right)^\xi\right)^\varsigma \tag{4}$$

with

$$T_{tr}(\dot{\overline{\varepsilon}}_p) = \vartheta_0 + \Delta\vartheta \cdot \ln\left(1+\frac{\dot{\overline{\varepsilon}}_p}{\dot{\varepsilon}_n}\right) \tag{5}$$

including the material constants ϑ_0, $\Delta\vartheta$, ξ, ς and the melting temperature T_m.

The modelling of the grain refinement bases on the Zener-Hollomon parameter Z. The Zener-Hollomon parameter Z depends on the plastic strain rate $\dot{\varepsilon}_{pl}$ and the temperature T. The validation of this approach is published in [16] for machining of AISI 4140.

3. Simulations and experiments

3.1. Simulations

The simulations of the mechanical surface modification during Complementary Machining are carried out in two series in order to identify the influence of the form-factor K on the resulting surface layer states. In series 1 the penetration depth a_p is constant at 20 µm and the surface modification velocity v_{st} varies from 20 to 150 m/min. The objective of this series is to identify the influence of the surface modification velocity on the process forces, with maximal temperatures and resulting grain size for AISI 4140.

In series 2 the surface modification velocity v_{st} is constant at 150 m/min and the influence of the penetration depth a_p was analyzed through a varying a_p from 10 to 40 µm. In series 2 AISI 4140 and Armco-Iron was investigated.

In both series during the mechanical surface modification the rake angle γ is held constant at -7°. Furthermore, three different microgeometries K = 0.2, 1 and 2 based on r_β = 40 µm were investigated. Tab. 1 shows the simulated parameters.

Table 1. Simulated process parameters and form-factors

Series		Surface modification velocity v_{st} [m/min]	Form-factor K [-]	Penetration depth a_p [µm]	Material
1	from	20	0.2	20	AISI 4140
	to	150	2		
2	from	150	0.2	10	Armco
	to		2	40	AISI 4140

3.2. Experiments

For calibrating the material model (Eq. 2 to 5) orthogonal cutting experiments were carried out on a Karl Klink vertical broaching machine. The workpiece was clamped vertically on the linear machine slide that moves upwards with the relative velocity v_{rel}. The length of the workpiece is l = 80 mm, the width w = 7 mm and thickness t = 4 mm. Uncoated cutting tools from Walter Tools (WKM P8TN 6028833) were used. The cutting edges microgeometries (form-factors K = 0.2, 1 and 2) were prepared by brushing and were measured using a Mahr perthometer. The process forces were measured by a Kistler three component dynamometer of Type Z 3393. Focused ion beam-technique was applied using a FEI Strata 400S Dual Beam FIB/SEM to study the microstructure. The ion channeling contrast imaging was performed by detecting secondary electrons emitted due to the irradiation of the cross-section area with an ion beam of 9 pA.

4. Results and discussion

4.1. Constant penetration depth a_p

For AISI 4140 Fig. 2 and 3 show the surface modification force F_{st} and passive force F_p for different surface modification velocities and form-factors K and for the penetration depth

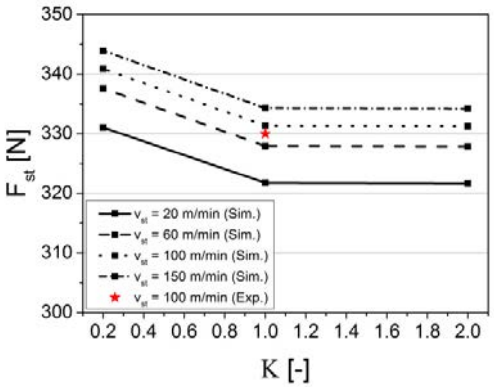

Figure 2. Surface modification force F_{st} for surface modification velocities v_{st} and penetration depth a_p of 20 µm for AISI 4140

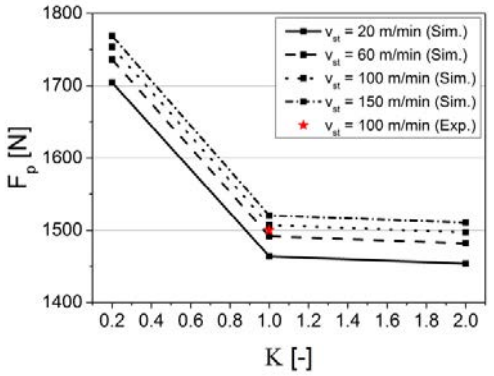

Figure 3. Passive force F_p for surface modification velocities v_{st} and penetration depth a_p of 20 µm for AISI 4140

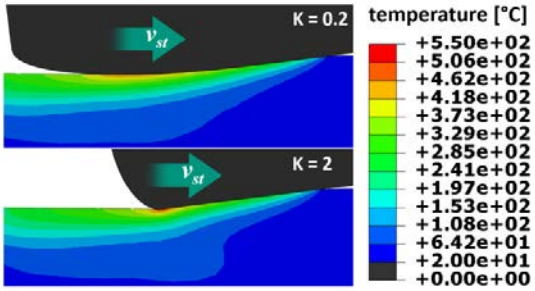

Figure 4. Temperature T of surface modification velocity v_{st} = 150 m/min and penetration depth a_p of 20 µm for AISI 4140

a_p = 20 µm. The results confirm the observation of previous studies. Process forces are slightly sensitive to an increased surface modification velocities [10, 11]. Regarding the influence of different form-factors, it can be observed that form-factors K < 1 lead to higher process forces. This can be compared to the results in [17] according to which dull cutting edges lead to higher process forces than sharp edges. Concerning the change of processing direction in Complementary Machining form-factors K < 1 are dull and cutting edge microgeometries K > 1 are sharp cutting edges. Between these two kinds of cutting edges huge differences in process forces can be observed whereas an increased form-

factor $K > 1$ has no more significant influence on process forces.

Fig. 4 shows the generation of heat during Complementary Machining of AISI 4140 for $a_p = 20$ µm and $K = 0.2$ and 2. It was determined that form-factors $K > 1$ cause locally concentrated higher temperatures than microgeometries $K < 1$ which heat a larger volume of material to a lower temperature.

In Fig. 5 the maximum temperature T is shown with a constant penetration depth $a_p = 20$ µm and varying surface modification velocities for AISI 4140. The results show that an increasing form-factor K results in an increasing process temperature. Furthermore, higher surface modification velocities cause higher temperatures. This can be explained by the influence of the surface modification velocity on the two sources of heat in the model, friction and plastic deformation. Both sources increase with higher surface modification velocity.

In Fig. 6 the resulting grain size g_s is shown related to the initial state after the surface modification by Complementary Machining was issued. The results show a great dependence of grain refinement on the temperature. As it is shown in Fig. 6 only high surface modification velocities ($v_{st} > 100$ m/min) lead to significant grain refinement. For this reason, simulations with a constant surface modification velocity $v_{st} = 150$ m/min were carried out in the second simulation series. There, the penetration depth a_p varied.

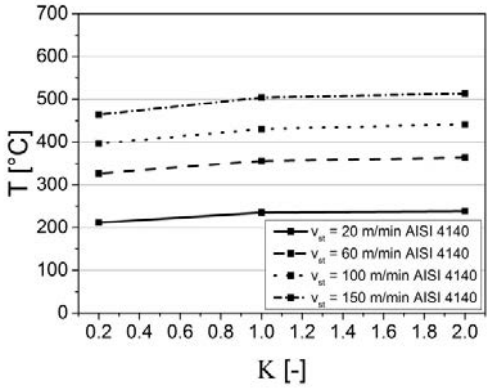

Figure 5. Maximal temperature T for surface modification velocities v_{st} and penetration depth a_p of 20 µm for AISI 4140

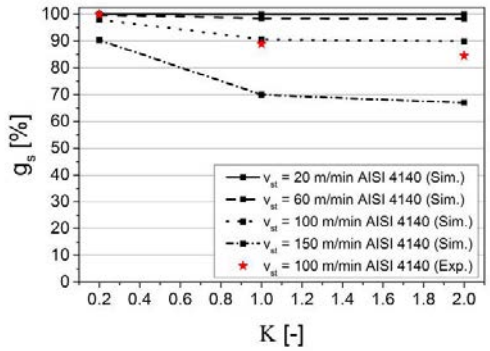

Figure 6. Grain size g_s for surface modification velocities v_{st} and penetration depth a_p of 20 µm for AISI 4140

4.2. Constant surface modification velocity v_{st}

In Fig. 7 and 8 the process forces of different form-factors K, different penetration depths a_p and surface modification velocity $v_{st} = 150$ m/min for Armco-Iron are presented. The results of the simulation show no significant influence of the form-factor K on process forces during the surface modification by Complementary Machining of Armco-Iron. As it was expected an increasing penetration depth a_p leads to higher process forces. Regarding the passive force F_p the form-factors $K < 1$ cause slightly higher passive forces than the form-factors $K > 1$. This can be explained by the increase of contact area using $K < 1$ which increases the area affected by the passive force.

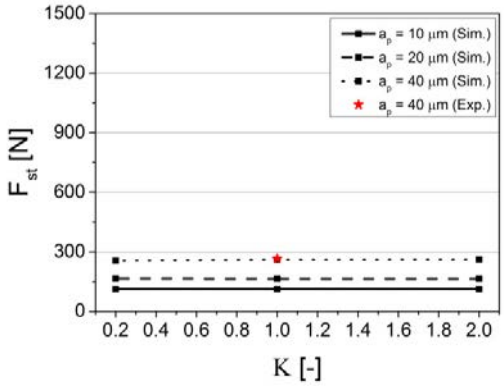

Figure 7. Surface modification force F_{st} for constant the surface modification velocity v_{st} of 150 m/min and different penetration depths a_p for Armco-Iron

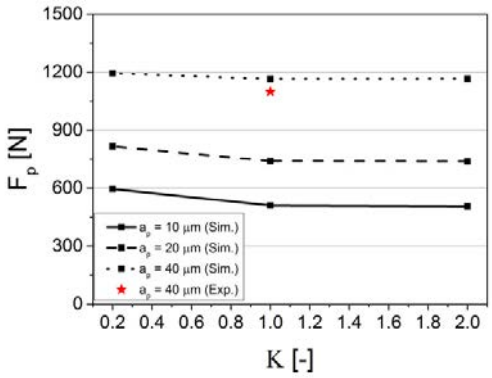

Figure 8. Passive force F_p for constant surface modification velocity v_{st} of 150 m/min and different penetration depths a_p for Armco-Iron

During Complementary Machining of Armco-Iron the results of process forces in general show similar dependencies as the results of AISI 4140 (Fig. 9 and 10). According to the results of Armco-Iron the form-factor K has a negligible influence on the surface modification force. However, the results for a form-factor $K > 0.2$ show that the passive force can be reduced and is constant for $K > 1$. This same tendency was observed during surface modification of Armco-Iron, though AISI 4140 is more sensitive to the influence of different form-factors K.

For AISI 4140 the process forces are twice as high as the process forces of Armco-Iron. The results of this simulation

study are in conformity with the experimental results of [10]. The effect is caused by the lower strength and higher ductility of Armco-Iron in comparison to AISI 4140.

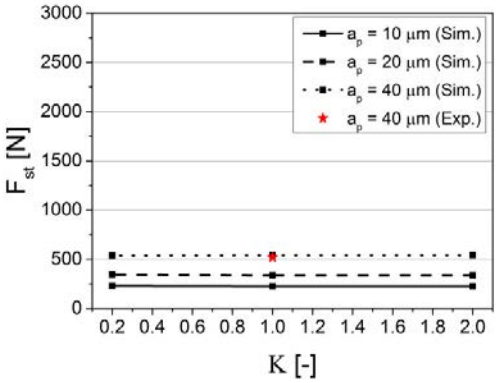

Figure 9. Surface modification force F_{st} for the constant surface modification velocity v_{st} of 150 m/min and different penetration depths a_p for AISI 4140

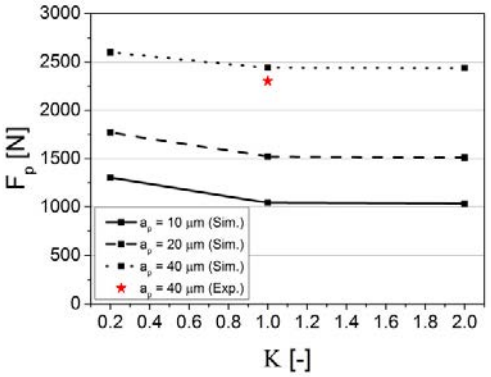

Figure 10. Passive force F_p for constant surface modification velocity v_{st} of 150 m/min and different penetration depths a_p for AISI 4140

In conclusion, the cutting edge microgeometry has a major influence on the passive force F_p compared to the surface modification force F_{st}.

Fig. 11 and 12 show the maximum temperature T for different form-factors K and penetration depths a_p using the surface modification velocity v_{st} = 150 m/min of Armco-Iron and AISI 4140. The results show that higher penetration depths a_p lead to higher temperatures according to higher plastic deformation. It is remarkable that form-factors $K > 0.2$ lead to lower passive forces and simultaneously increases thermal load. Whereas form-factors $K < 1$ cause higher passive forces along with decreasing thermal load. During the surface modification of AISI 4140 in comparison to Armco-Iron, a considerable higher amount of heat is generated because of the higher mechanical work needed. The higher strength of AISI 4140 compared to Armco-Iron causes a much higher amount of heat through plastic deformation.

Fig. 13 shows the resulting grain refinement during Complementary Machining of AISI 4140 with form-factors K = 0.2 and 2, v_{st} = 150 m/min and penetration depth a_p = 40 µm. through form-factors $K > 1$ smaller grain sizes are achievable with equal penetration depth and surface treatment velocity.

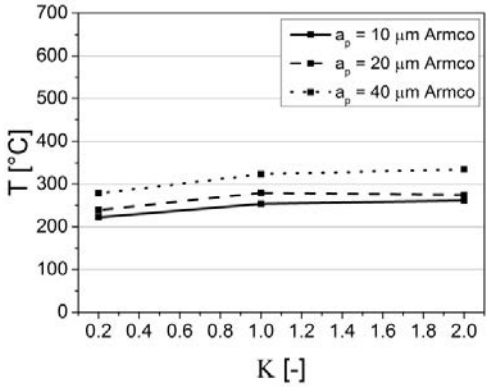

Figure 11. Maximal temperature T for constant surface modification velocity v_{st} of 150 m/min and different penetration depths a_p for Armco-Iron

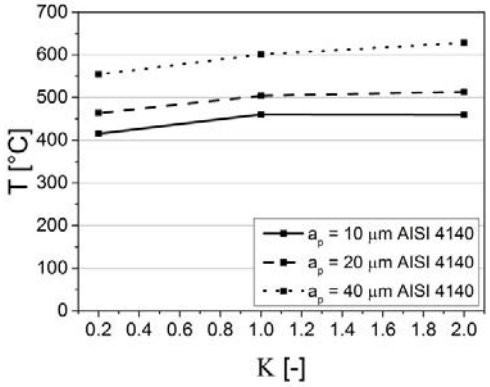

Figure 12. Maximal temperature T for constant surface modification velocity v_{st} of 150 m/min and different penetration depths a_p for AISI 4140

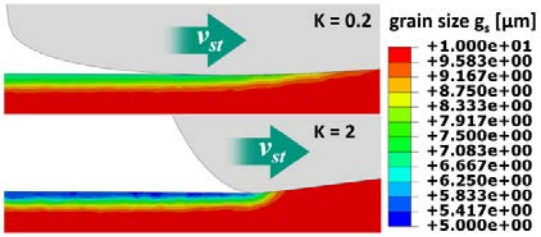

Figure 13. Resulting grain size g_s for form-factor K = 0.2 and 2, surface modification velocitiy v_{st} = 150 m/min and penetration depths a_p = 40 µm for AISI 4140

The grain refinement of different form-factors K and penetration depths a_p is shown in Fig. 14. The results of the simulations suggest insignificant grain refinement after machining of Armco-Iron. This is caused by the significant lower temperatures especially in comparison to the resulting process temperatures of AISI 4140. As observed before, under the given constraints grain refinement is mostly depending on temperature. Form-factors $K > 1$ cause higher temperatures than $K < 1$. Consequently, it results in a smaller grain size. Because form-factors $K < 1$ cause less heat through plastic straining, lower temperatures and consequently less grain refinement is achieved.

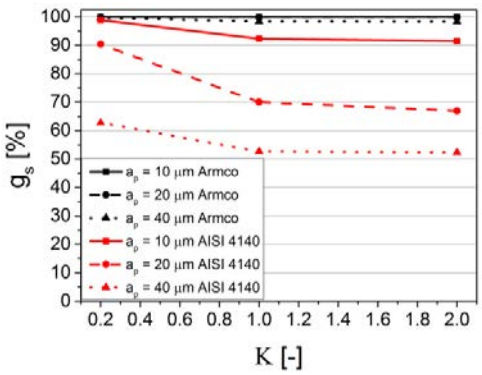

Figure 14. Resulting grain size g_s based on the initial grain size for constant surface modification velocity v_{st} of 150 m/min and different penetration depths a_p for AISI 4140 and Armco-Iron

5. Conclusion and outlook

In this paper the influence of the cutting edge microgeometry (form-factor *K*) and surface modification velocity v_{st} on process forces, maximal temperatures and resulting grain size during the mechanical surface modification by Complementary Machining of AISI 4140 and Armco-Iron was examined with a 3D-FEM-simulation in ABAQUS/Standard. During the mechanical surface modification of AISI 4140 the simulated process forces correspond to experimental values of previous investigations and are twice as high as the process forces during the surface modification of Armco-Iron.

It has been shown that a sensitivity of the form-factor *K* on the process forces, maximal temperatures and resulting grain size exists. However, the potential of the form-factor on resulting process forces, maximal temperatures or resulting grain sizes depends on the workpiece material. So the influence is more pronounced during the surface modification of ASIS 4140 compared to Armco-Iron.

In further investigations, an optimal cutting edge microgeometry for the complete process strategy Complementary Machining will be identified. To estimate the thermo-mechanical load the FEM-simulation will be used.

Acknowledgements

The authors thank the German Research Foundation (DFG) for the funding of the research project.

References

[1] Roland T, Retraint D, Lu K, Lu J. Fatigue life improvement through surface nanostructuring of stainless steel by means of surface mechanical attrition modification. Scripta Materialia 2006;54:1949–1954.
[2] Schulze V. Modern mechanical surface modification: states, stability, effects. Wiley-VCH , Weinheim, 2006.
[3] Ball A. On the importance of work hardening in the design of wear-resistant materials. Wear 1983;91:201–207.
[4] Hassan AM, Momani AM. Further improvements in some properties of shot peened components using the burnishing process. Int. J. Mach. Tools Manuf 2000;40:1775–1786.
[5] Amanov A, Cho IS, Pyoun YS, Lee CS, Park IG. Micro-dimpled surface by ultrasonic nanocrystal surface modification and its tribological effects. Wear 2012;286:136–144.
[6] Denkena B, Biermann D. Cutting edge geometries. CIRP Annals - Manufacturing Technology 2014;63:631-653.
[7] Basset E. Belastungsspezifische Auslegung und Herstellung von Schneidkanten für Drehwerkzeuge. Leibnitz Universität Hannover, Dissertation, 2014.
[8] Rehe M. Herleitung prozessbezogener Kenngrößen der Schneidkantenverrundung im Fräsprozess. Leibnitz Universität Hannover, Dissertation, 2015.
[9] Segebade E, Zanger F, Schulze V. Influence of different asymmetrical cutting edge microgeometries on surface integrity. Procedia CIRP 2016;45:11-14.
[10] Zanger F, Gerstenmeyer M. Material Behaviour of Armco-Iron and AISI 4140 at High Speed Deformation during Machining. Advanced Materials Research 2014;1018:161-166.
[11] Gerstenemyer M, Zanger F, Volker S. Complementary Machining – Machining Strategy for Surface Modification. Procedia CIRP 2016;45247-250.
[12] Denkena B, Reichstein M, Brodehl J, Leon Garcia L. Surface Preparation, Coating and Wear Performance of Geometrically Defined Cutting Edges. 8th CIRP Int. Workshop on Modeling of Machining Operations, May 10-11 2005 (Chemnitz).
[13] Tomé CN, Canova GR, Kocks UF, Christodoulou N, Jonas J. The relationship between macroscopic and microscopic strain hardening in F.C.C. polycrystals. Acta metallurgica 1984;32:1637-1653.
[14] Voce E. The relationship between stress and strain for homogeneous deformation. Journal of the Institute of Metals 1948;74:537-562.
[15] Authenrieth H. Numerische Analyse der Mikrozerspanung am Beispiel von normalisiertem C45E. Karlsruhe Institute of Technology, Dissertation, 2010.
[16] Ambrosy F, Zanger F, Schulze V. FEM-simulation of machining induced nanocrystalline surface layers in steel surface prepared für tribological applications. CIRP Annals – Manufacturing Technology 2015;64:69-72
[17] Denkena B, Köhler J, Mesfin Sisay Mengesha. Influence of the cutting edge rounding on the chip formation process: Part 1. Investigation of material flow, process forces, and cutting temperature. Production Engineering 2012;6;4:329-338.